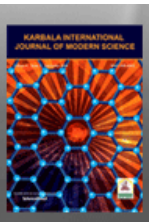

Karbala International Journal of Modern Science

Volume 7 | Issue 4 Article 12

Calculation and comparison of certain physical properties of sample irregular galaxies with the Milky Way galaxy

Hasanain Hassan AL-Dahlaki MSc
Department of Astronomy and Space, College of science, University of Baghdad, Iraq,
hasanain.ali@sc.uobaghdad.edu.iq

Follow this and additional works at: https://kijoms.uokerbala.edu.iq/home

 Part of the Biology Commons, Chemistry Commons, Computer Sciences Commons, and the Physics Commons

Recommended Citation

AL-Dahlaki, Hasanain Hassan MSc (2021) "Calculation and comparison of certain physical properties of sample irregular galaxies with the Milky Way galaxy," *Karbala International Journal of Modern Science*: Vol. 7 : Iss. 4 , Article 12.
Available at: https://doi.org/10.33640/2405-609X.3163

This Research Paper is brought to you for free and open access by Karbala International Journal of Modern Science. It has been accepted for inclusion in Karbala International Journal of Modern Science by an authorized editor of Karbala International Journal of Modern Science.

University of Kerbala

Calculation and comparison of certain physical properties of sample irregular galaxies with the Milky Way galaxy

Abstract

Irregular galaxies often include a mix of old and young celestial populations, as well as dust and gas. This study makes an early effort at the morphological classification of irregular galaxies. These sources have been chosen from (70) irregular galaxies data samples from a Catalogue survey. We present a statistical analysis of the physical properties for the chosen data from the database and a collection of tools that used to study the physics of galaxies and cosmology HYPERLEDA (http://atlas.obshp.fr/hyperleda/) and NASA /IPAC Extragalactic Database NED (https://ned.ipac.caltech.edu/) survey.

Creative Commons License

This work is licensed under a Creative Commons Attribution-Noncommercial-No Derivative Works 4.0 License.

This research paper is available in Karbala International Journal of Modern Science: https://kijoms.uokerbala.edu.iq/home/vol7/iss4/12

1. Introduction

Galaxies are the fundamental building elements of the universe. Few of these galaxies were just structurally simple, usually contain only standard stars as well as exhibiting no specific physical characteristics, the others are complicated structures, constructed from several different interacts on stars, neutral and ionized gas components [1]. Galaxies may typically range from dwarf galaxies with tens of millions of stars to massive galaxies with trillions of stars. Aside from their varied sizes, galaxies have a variety of shapes [2].

A previous study by Mirjana P [3]. Illustrated that there is still a reasonable understanding of many characteristics of different types of galaxies, especially when moving to high redshifts. Mostly, galaxies that are understood emerge from the light that is detected. This variable (light) includes a large number of details from the source produced via it, like (mass, distance, age, and type, etc.) following Rashed et al. [4] that studied the flux density of active galaxies bright at different spectral bands.

A few irregular galaxies have fairly predictable rotation curves because others show impossible-to-spin objects. Some authors [5] studied the results of a simple derivation, which is similar to the more exact value obtained via stellar structure equations for the degenerate matter.

Because stars do not revolve at the same rate around the galactic center, this study will investigate the gravitational force that results when recognizing where mass has transported. This work might reveal how the positions and speeds of stars and galaxies change throughout time [6].

The morphological categorization of galaxies is an intriguing issue for investigating the fundamentals of galaxy assembly. Early-type galaxies (ETGs) include elliptical and lenticular galaxies, and late-type galaxies, which contain spiral and irregular galaxies, are the two major kinds. The primary types of galaxies in the observable universe are those distinct sorts [7].

The types of morphological galaxies might lead to significant studies of astrophysical factors. Every model of galaxy structure and evolution had to include the spectrum of forms observed [8].

According to a published article, a previous study [9] measures the magnitude of pressure support; provided by the HI velocity dispersion in the SHIELD galaxies. They discovered that this aspect can be significant for low-mass systems. So they adjust the enclosed dynamical mass to account for the HI velocity dispersion contribution [10], the most interesting findings of this research are that the surface density of baryonic mass in galaxies' outer disks can be lower than the dynamical mass surface density, implying that there isn't sufficient baryonic mass (in the form of stars and HI gas). They found that this may mean one of two things: (i) the luminosity stellar mass in the outer disks is low due provides HI disks upright, (ii) dark matter is correlated with the disk.

This paper focuses on sections; are arranged as follows: section one outlines the mathematical analyses associated, with our project, determining the structure used in the statistical analysis with the parameter inferences that have been calculated in this paper. Section three: showing determined results, likewise, measurable investigation of the used sample data. In extension, the relationship between the obtained parameters will discuss in this section. As well as we will be investigating these correlations.

1.1. The sample, data, and derived parameters

This paper was presented a scientific analysis of (70) samples of irregular galaxies and these samples have taken from HYPERLEDA (http://atlas.obs-hp.fr/hyperleda/) and NED (https://ned.ipac.Caltech.edu/) surveys as shown in Table 1 column 4. Late-type irregular galaxies picked from the analysis and augmented by galaxies, including their earlier Hubble classification with absolute magnitudes of less than $M_B = -17^{mag}$. Also, we picked out galaxies with HI flux densities greater than 200 mJy and Galactic latitudes $\lceil b \rceil > 10^{10}$. This result is about (70) samples of irregular galaxies, as shown in Tables 1 and 2.

1.2. Data used

A lot of galaxies are investigated lengthy to expand the radius of the first grate band. It includes the recorded data in a single 12-h synthesis analysis, and measurement was recording using a velocity distribution taper and a stream width of 2 or 4 km s^{-1} [11].

It's worth noting that determining the mass may need knowledge of the star's or gases' spectral rotation velocity. The calculations of this selected data will assist in the current study to explain the proportion

https://doi.org/10.33640/2405-609X.3163
2405-609X/© 2021 University of Kerbala. This is an open access article under the CC BY-NC-ND license (http://creativecommons.org/licenses/by-nc-nd/4.0/).

Table 1
The sample and parameters of irregular galaxies.

Name (1)	Other Name (2)	Morpholog-ical type (3)	log d_{25} (arcmin) (4)	d_{25} (arcmin) (5)	V_H (km/s) (6)	D (Mpc) (7)	Ao (Kpc) (8)	M_I (M_Θ) (9)
UGC 5272	UGC 0947	IB	1.21	1.62181	520	7.428571	2.528458	70,352,827
UGCA 320	DDO 161	IB	1.83	6.76083	743	10.6143	15.06058	7.51E+09
UGC 4305	Holmberg II	Im	1.9	7.943282	158	2.257143	3.762785	8.24E+08
UGC 5414	NGC 3104	IAB	1.48	3.019952	604	8.628571	5.468765	3.53E+09
UGC 5829	PGC 31923	Im	1.65	4.466836	629	8.985714	8.423701	1.04E+10
UGC 6923	PGC 37553	IAB	0.98	0.954993	1085	15.5	3.106577	5.4E+09
UGC 7232	NGC 4190	IB	1.18	1.513561	158	2.257143	0.716984	2.97E+08
UGC 7278	NGC 4214	Im	1.83	6.76083	292	4.171429	5.918821	2.51E+09
UGC 7690	PGC41576	Im	1.14	1.380384	531	7.585714	2.197591	2.35E+09
UGC 9992	PGC 55809	Im	1.16	1.44544	428	6.114286	1.854796	2.68E+08
UGCA444	PGC000143	IB	2.02	10.47129	111	1.585714	3.484779	5.86E+08
UGC 7648	NGC 4485	IB	1.3	1.995262	483	6.9	2.889345	4.32E+09
UGC 8303	DDO 166	IAB	1.16	1.44544	945	13.5	4.095285	1.82E+09
UGC 9219	NGC 5608	IB	1.22	1.659587	666	9.514286	3.313802	1.76E+08
UGC 06403	NGC 3656	I0	1.16	1.44544	2871	41.01429	12.44187	1.21E+11
NGC 3952	IC 2972	IBm	1.21	1.62181	1577	22.52857	7.668034	9.88E+09
UGC 8847	NGC 5363	I0	1.62	4.168694	1134	16.2	14.17312	4.35E+11
UGC12048	NGC 7292	IBm	1.26	1.819701	986	14.0857	5.379338	1.91E+09
UGC 12885	NGC 7800	IB	1.24	1.737801	1750	25	9.117806	1.54E+09
IC 4662	PGC 60851	IBm	1.32	2.089296	306	4.371429	1.916787	77,409,079
NGC 6822	DD 209	IB	2.19	15.48817	56	0.8	2.600401	5.44E+08
UGC 3851	NGC 2366	IB	1.64	4.365158	100	1.428571	1.308737	47,526,941
UGC 3056	NGC 1569	IB	1.59	3.890451	95	1.357143	1.108092	42,143,874
UGC 4459	DDO 53	Im	0.9	0.794328	24	0.342857	0.057156	123732.9
AGC 668	DDO 8	IB	2.26	18.19701	232	3.314286	12.65728	2.23E+08
UGC 2455	NGC 1156	IB	1.47	2.951209	373	5.328571	3.300359	1.73E+08
UGC 7074	NGC 4068	IAm	1.28	1.905461	210	3	1.199697	21,427,190
PGC 45717	ESO 269-58	I0	1.52	3.311311	400	5.714286	3.971114	89,323,073
NGC 5237	PGC 48139	I0	1.37	2.344229	361	5.157143	2.537228	83,725,498
UGCA 86	PGC 14241	Im	1.66	4.570882	71	1.014286	0.972995	88,412,026
NGC 1427A	PGC 13500	IB	1.36	2.290868	2026	28.94286	13.91527	6.87E+08
UGC 00668	AGC 00668	IB	2.26	18.19701	232	3.314286	12.65728	2.23E+08
PGC 006430	ESO 245-G005	IBm	1.52	3.311311	394	5.628571	3.911547	4.94E+08
UGC 04305	PGC 023324	Im	1.9	7.943282	158	2.257143	3.762785	82,417,203
UGC 7068	NGC 4080	Im	1.09	1.230269	558	7.971429	2.058195	2.29E+08
UGC 3711	NGC 2337	IB	1.34	2.187762	436	6.228571	2.859821	5.29E+08
UGC 5151	PGC 027602	Irr	0.82	0.660693	771	11.01429	1.527238	2.45E+08
NGC 5408	PGC 050073	IB	1.45	2.818383	506	7.228571	4.275657	1.01E+08
IC 4870	PGC 063432	IBm	1.22	1.659587	877	12.52857	4.36367	1.34E+08
IC 5152	PGC 067908	IAB	1.71	5.128614	124	1.771429	1.906663	1.13E+08
UGC 11891	PGC 067946	Im	1.52	3.311311	461	6.585714	4.576708	8.57E+08
UGC 192	IC 10	IB	1.83	6.76083	345	4.928571	6.993127	4.78E+08
UGC 4305	DDO 50	Im	1.9	7.943282	158	2.257143	3.762785	82,417,203
UGC 1200	PGC006309	IB	1.13	1.348963	812	11.6	3.284039	2.81E+08
NGC 1140	PGC 10966	IBm	1.31	2.041738	1501	21.44286	9.188254	1.71E+09
NGC 1427A	PGC013500	IB	1.36	2.290868	2026	28.94286	13.91527	6.87E+08
NGC 1800	PGC 016744	IBm	1.19	1.548817	804	11.48571	3.733433	2.6E+08
NGC 2915	PGC 026761	I0	1.26	1.819701	465	6.642857	2.536911	3.51E+08
UGC 07000	PGC037914	IB	0.94	0.870964	1487	21.24286	3.882963	3.04E+08
UGC 8009	NGC 4753	I0	1.81	6.456542	1243	17.75714	24.06154	4.47E+10
UGC 2023	DDO 25	Im	1.41	2.570396	603	8.614286	4.646967	4.42E+08
UGC 5637	NGC3239	IB	1.56	3.630781	752	10.74286	8.18597	1.83E+09
UGC 6670	PGC 1556477	IB	1.18	1.513561	925	13.21429	4.197532	9.66E+08
UGC 8303	DDO166	IAB	1.16	1.44544	945	13.5	4.095285	1.82E+08

(*continued on next page*)

Table 1 (*continued*)

Name (1)	Other Name (2)	Morpholog-ical type (3)	log d_{25} (arcmin) (4)	d_{25} (arcmin) (5)	V_H (km/s) (6)	D (Mpc) (7)	Ao (Kpc) (8)	M_I (M_Θ) (9)
UGC 1547	DDO 17	IBm	1.3	1.995262	2643	37.75714	15.81064	2.03E+10
UGC 75	PGC 000647	IB	1.18	1.513561	865	12.35714	3.92526	1.75E+08
UGC03647	DDO 40	Ibm	1.03	1.071519	1386	19.8	4.452619	69,275,986
UGC03860	DDO 43	IB	1.13	1.348963	344	4.914286	1.391268	9,392,756
UGCA205	DDO 75	IB	1.72	5.248075	324	4.628571	5.097971	1.23E+08
UGC 5373	DDO 70	IB	1.69	4.897788	301	4.3	4.419965	33,163,549
IC 1613	PGC 003844	IB	2.26	18.19701	232	3.314286	12.65728	2.23E+08
AGC 2455	PGC 11329	IB	1.47	2.951209	373	5.328571	3.300359	1.73E+08
NGC 2010	PGC 017793	IB	1.09	1.230269	1193	17.04286	4.400406	2.11E+08
UGC 6565	NGC 3738	Im	1.36	2.290868	224	3.2	1.53851	1.03E+08
UGC 1438	NGC 746	Im	1.26	1.819701	705	10.07143	3.846285	3.17E+08
UGC 5935	PGC 032434	IBm	1.49	3.090295	1694	24.2	15.69516	2.13E+09
UGC 6016	PGC032740	Im	1.26	1.819701	1512	21.6	8.249053	1.25E+09
UGC 6024	NGC 3448	I0	1.47	2.951209	1372	19.6	12.13966	4.41E+09
UGC 5995	NGC 4032	IBm	1.13	1.348963	1270	18.14286	5.136367	6.25E+08
UGC 12060	PGC069019	IB	1.04	1.096478	884	12.62857	2.90606	1.98E+08

Table 2
Some physical properties of Irregular Galaxies.

NAME (1)	btc (mag) (2)	V_{rot} (Km/s) (3)	f_{60} (Jy) (4)	f_{100} (Jy) (5)	L_{fir} (L_Θ) (6)	L_{opt} (L_Θ) (7)
UGC 5272	13.2	33.7	0.2168	0.4926	2.3E+07	5E+07
UGCA 320	11.74	45.1	0.3979	0.787	8.1E+07	4E+08
UGC 4305	10.74	29.9	1.147	2.616	1.1E+07	4E+07
UGC 5414	13.44	51.3	0.3692	1.003	5.7E+07	5E+07
UGC 5829	13.56	71.1	0.2388	0.7613	4.4E+07	5E+07
UGC 6923	13.53	84.2	0.3725	0.9043	1.8E+08	1E+08
UGC 7232	13.65	41.1	0.3658	1.208	4,319,256	3E+06
UGC 7278	9.91	41.6	0.3658	1.208	14752.3	3E+08
UGC 7690	12.89	66.1	0.535	1.209	5.9E+07	6E+07
UGC 9992	14.85	24.3	0.09	0.26	7,249,854	7E+06
UGCA444	10.01	26.2	0.32	1.04	1,848,267	4E+07
UGC 7648	11.91	78.1	2.16	3.83	1.8E+08	1E+08
UGC 8303	13.27	42.6	0.3796	1.2	1.6E+08	1E+08
UGC 9219	13.33	46.6	0.1956	0.49	3.5E+07	7E+07
UGC 06403	12.96	199.2	2.333	5.442	7.6E+09	2E+09
NGC 3952	12.27	72.5	1.502	2.077	1.2E+09	1E+09
UGC 8847	10.88	353.9	1.65	5	9.6E+08	2E+09
UGC12048	12.47	38.1	1.167	2.725	4.1E+08	3E+08
UGC 12885	12.42	83.1	1.249	2.552	7.8E+09	1E+09
IC 4662	10.76	40.6	8.138	11.83	1E+08	1E+08
NGC 6822	8.31	92.4	7.9	11.2	7,963,717	5E+07
UGC 3851	10.52	38.5	3.513	4.668	1.1E+07	2E+07
UGC 3056	8.31	39.4	45.41	47.29	1.2E+08	1E+08
UGC 4459	14.3	9.4	0.278	0.48	55450.3	34,932
AGC 668	9.85	26.8	1.42	3.69	3.2E+07	2E+08
UGC 2455	10.9	46.3	6.16	9.202	2.8E+08	2E+08
UGC 7074	12.57	27	0.2278	0.8336	5,040,015	1E+07

(*continued on next page*)

Table 2 (*continued*)

NAME (1)	btc (mag) (2)	V_{rot} (Km/s) (3)	f_{60} (Jy) (4)	f_{100} (Jy) (5)	L_{fir} (L_{Θ}) (6)	L_{opt} (L_{Θ}) (7)
PGC 45717	12.24	30.3	0.43	1.6	3.5E+07	6E+07
NGC 5237	12.79	36.7	0.36	0.55	1.5E+07	3E+07
UGCA 86	9.1	60.9	1.043	4.979	3,108,915	4E+07
NGC 1427A	12.97	44.9	0.2073	0.7782	4.3E+08	8E+08
UGC 00668	9.85	26.8	1.42	3.69	3.2E+07	2E+08
PGC 006430	12.68	71.8	0.2242	0.5961	1.5E+07	4E+07
UGC 04305	10.74	29.9	1.147	2.616	1.1E+07	4E+07
UGC 7068	13.18	67.4	0.2863	1.037	4.4E+07	5E+07
UGC 3711	12.4	86.9	1.659	3.213	1.1E+08	7E+07
UGC 5151	13.5	80.9	0.5642	1.112	1.2E+08	8E+07
NGC 5408	11.4	31.1	2.825	2.958	2.1E+08	2E+08
IC 4870	13.59	35.4	0.713	2.308	2.6E+08	9E+07
IC 5152	10.01	49.2	2.461	6.861	1.6E+07	5E+07
UGC 11891	13.63	87.4	0.966	3.899	1.1E+08	2E+07
UGC 192	11.78	52.8	2.265	1.28	6.8E+07	7E+07
UGC 4305	10.74	29.9	1.147	2.616	1.1E+07	4E+07
UGC 1200	13.53	59.1	0.2875	0.8992	8.7E+07	8E+07
NGC 1140	12.04	87.2	3.358	4.922	2.5E+09	1E+09
NGC 1427A	12.97	44.9	0.2073	0.7782	4.3E+08	8E+08
NGC 1800	12.82	53.3	0.7679	1.82	2E+08	2E+08
NGC 2915	11.7	75.2	0.889	1.688	6.9E+07	1E+08
UGC 07000	13.78	56.5	0.3571	0.9529	3.3E+08	2E+08
UGC 8009	10.41	275.4	2.438	9.008	1.9E+09	3E+09
UGC 2023	13.54	62.3	0.3144	0.7851	4.7E+07	4E+07
UGC 5637	11.31	95.6	3.421	6.405	6.9E+08	5E+08
UGC 6670	12.57	96.9	0.6878	1.609	2.3E+08	3E+08
UGC 8303	13.27	42.6	0.3796	1.2	1.6E+08	1E+08
UGC 1547	13.97	228.8	0.307	0.7954	8.9E+08	6E+08
UGC 75	12.35	42.6	0.7217	1.898	2.3E+08	3E+08
UGC03647	14.02	25.2	0.2011	0.7536	2E+08	2E+08
UGC03860	14.43	16.6	0.1	0.25	4,833,712	6E+06
UGCA205	11.99	31.4	0.2554	0.6738	1.1E+07	5E+07
UGC 5373	11.4	17.5	0.31	0.54	9,760,523	8E+07
IC 1613	9.85	26.8	1.42	3.69	3.2E+07	2E+08
AGC 2455	10.9	46.3	5.173	9.202	2.5E+08	2E+08
NGC 2010	12.94	44.2	0.6955	1.276	3.5E+08	3E+08
UGC 6565	11.24	52.3	2.003	3.523	3.5E+07	5E+07
UGC 1438	12.99	58	0.669	1.632	1.3E+08	1E+08
UGC 5935	11.73	74.4	6.15	9.56	5.9E+09	2E+09
UGC 6016	15.77	78.6	0.5	0.5	3.3E+08	4E+07
UGC 6024	11.55	121.7	5.865	10.65	3.9E+09	1E+09
UGC 5995	12.68	70.5	6.15	9.56	3.3E+09	4E+08
UGC 12060	14.48	52.7	0.2725	0.9315	1E+08	4E+07

Table 3
Comparison of Some physical properties between our work of Irregular Galaxies and our Galaxy (Milky Way).

Parameter	A_0 (Kpc)	M_I ($M_{\odot}$)	V_H km s^{-1}	Btc	V_{rot} km	Lfir L_{Θ}	Lopt L_{Θ}
Milky way	33.6[1]	1.5-8.5 $\times$ 10^{11}[1]	229[22]	20.3[22]	24[1]	8 $\times$ 10^{9}[23]	3 $\times$ 10^{9} [23]
Irregular Galaxies	5.664258	9.96 $\times$ 10^{9}	740.43	12.2	64.4	6 $\times$ 10^{8}	3 $\times$ 10^{8}

Table 4
Correlations coefficients Marked correlations are significant at p < .05000 N = 70, Means & Std.Dev.

	Means	Std.Dev.	Log L_{OPT}	Log L_{FIR}	Log A_0	Log Vrot^2	log M_I
Log L_{OPT}	9.035040	0.746004	1.000000	0.757240	0.474408	0.608691	0.702372
Log L_{FIR}	7.894329	1.029273	0.757240	1.000000	0.382888	0.620982	0.558827
Log A_0	0.647751	0.329477	0.474408	0.382888	1.000000	0.283993	0.469316
Log Vrot^2	3.428298	0.538726	0.608691	0.620982	0.283993	1.000000	0.815085
log M_I	8.653811	0.955864	0.702372	0.558827	0.469316	0.815085	1.000000

Table 5
Mean (average) variables and standard error for sample irregular galaxies.

	Valid N	Mean	Std.Dev.	Standard Error
Log L_{OPT}	70	9.035040	0.746004	0.089164
Log L_{FIR}	70	7.894329	1.029273	0.123022
Log A_0	70	0.647751	0.329477	0.039380
Log Vrot^2	70	3.428298	0.538726	0.064390
log M_I	70	8.653811	0.955864	0.114248

between some physical qualities of the investigated galaxies and the Milky Way's physical attributes.

1.3. The distance (D)

Understanding the structures that galaxies create and the activities; that occur inside them requires determining the distances between them. More than that, only distance gives the scientific framework for determining galaxies' distances. In astronomy, distances are being calculated using a set of essential object types, and we can now estimate distances on a scale of a few parsecs [12].

The distances of the selected galaxies in our sample are shown in Table 1. Here D is calculated from the systematic velocity of HI, with the embraced Hubble constant of $H_0 = 70 kms^{-1} Mpc^{-1}$ [13,14]. So, we calculate the distance to the galaxy in the unit (Mpc) that is calculated from Hubble's law, which is taken from Ref. [13]:

$$D = \frac{V_H}{H_0} \tag{1}$$

where V_H is Mean Heliocentric radial velocity in a unit (Km/s).

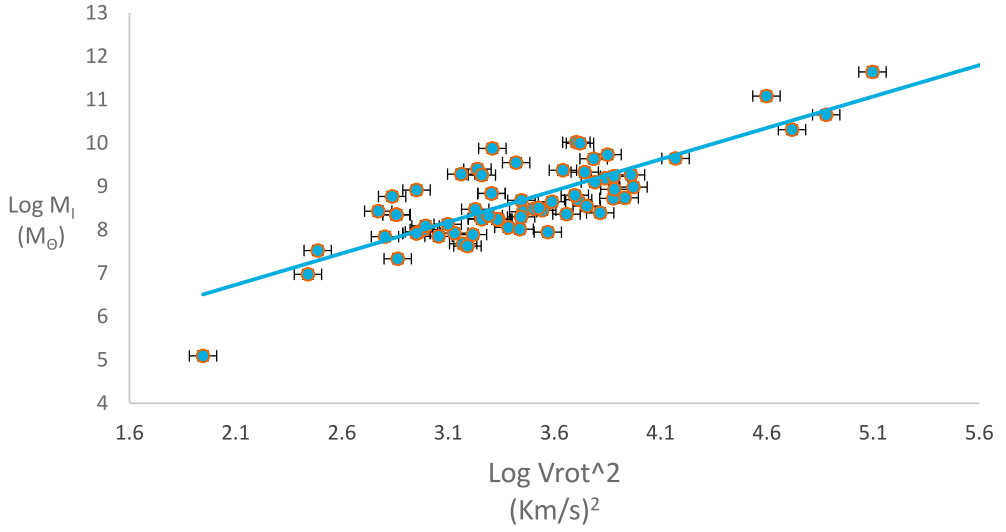

Fig. 1. Maximum rotation velocity $(V_{rot})^2 (km/s)^2$ as function of total mass $M_I(M_\odot)$ of sample Irregular galaxies with error bars.

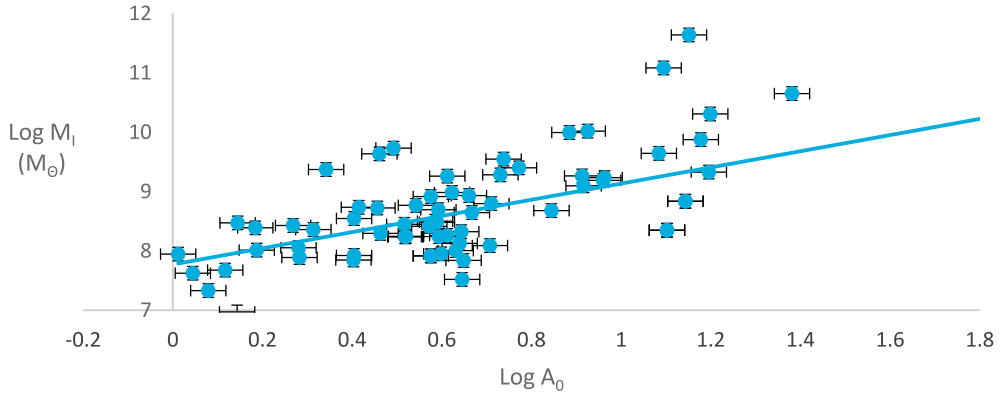

Fig. 2. Linear diameter $LogA_0(Mpc)$as a function of total mass $logM_I(M_\odot)$ of sample Irregular galaxies with error bars.

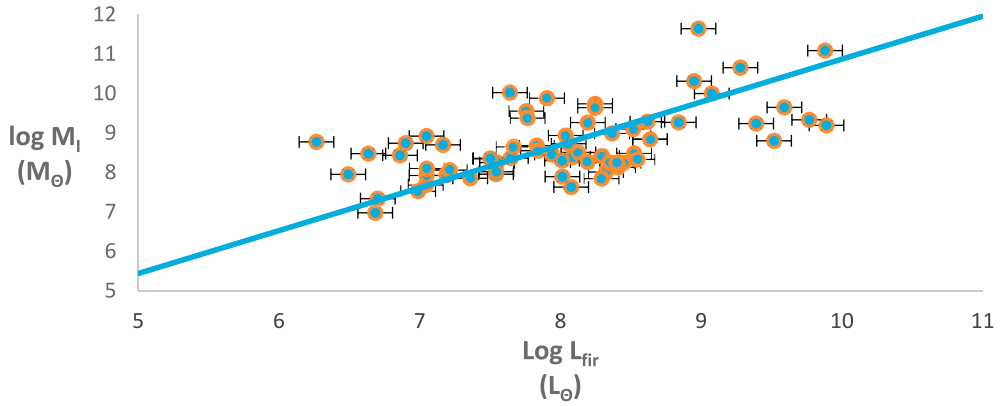

Fig. 3. **Far** infrared luminosity $LogL_{fir}(L_\Theta)$ as a function of total mass $logM_I(M_\odot)$ of sample Irregular galaxies with error bars.

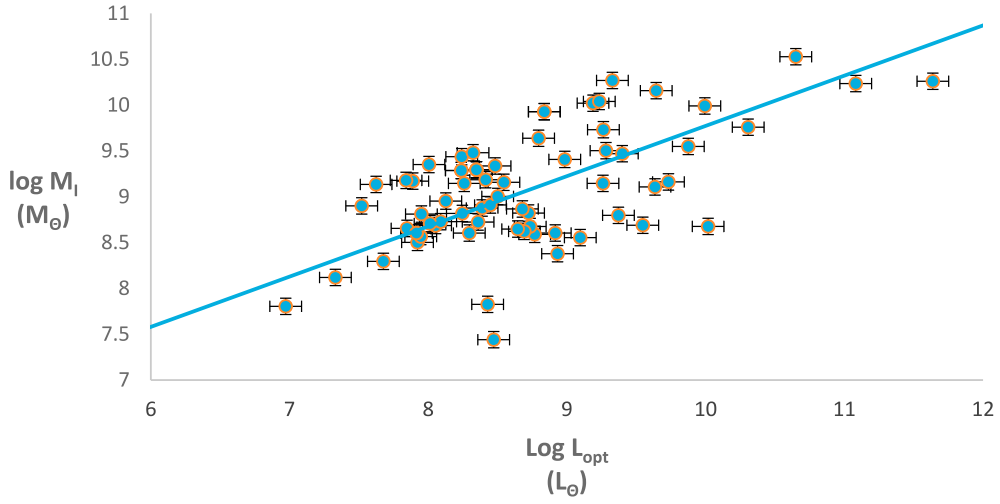

Fig. 4. Optical luminosity $LogL_{opt}(L_\Theta)$ as a function of total mass $logM_I(M_\odot)$ of sample Irregular galaxies with error bars.

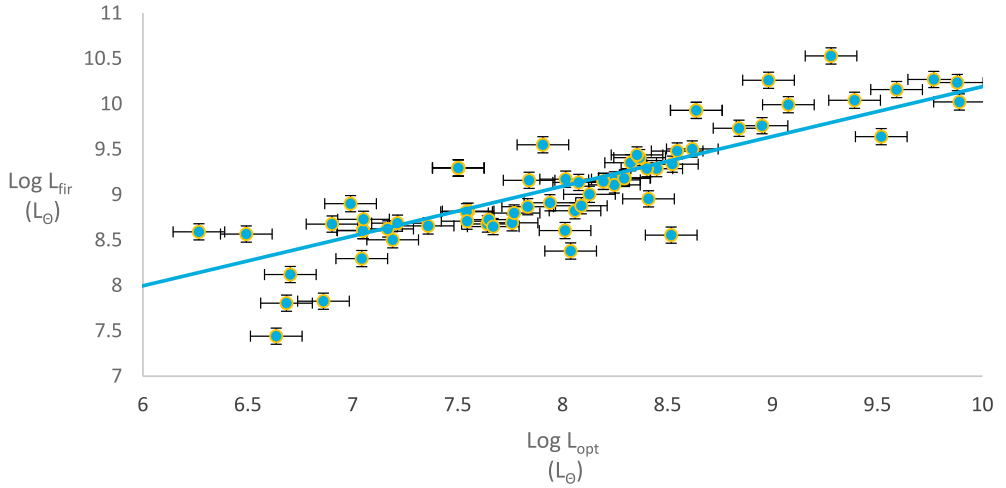

Fig. 5. Optical luminosity $LogL_{opt}(L_{\Theta})$ as a function of far infrared luminosity $LogL_{fir}(L_{\Theta})$ of sample Irregular galaxies with error bars.

1.4. Total mass of galaxies

We calculated the total mass of the galaxy in the unit (M_{Θ}) from Ref. [15]:

$$M_I = 2.45 \times 10^4 A_0 (\Delta v_{20} / \sin i) \quad (2)$$

At which time width at 20 percent peak maximum density in ($km.\ sec^{-1}$) is ($\Delta\upsilon_{20}$), and (i) is the inclination in degree (^{0}).

If a strictly circular motion of galaxies that assumed for an isolated system, the maximum rotational velocity ($V_{max} = \Delta\upsilon_{20}/\sin\ i$). The above equation (2) becomes [16]:

$$M_I = 2.45 \times 10^4 A_0 (V_{max})^2 \quad (3)$$

where A_0 is the linear diameter of galaxies in unit Kpc, we estimate the value $A_0$from Ref. [16], and all these parameter is shown in Table 1.

$$A_0 = 0.29087 \times d_{25} \times D \quad (4)$$

The dynamical mass ($\frac{GM_r}{r^2} = V_{rot}^2 - \sigma^2$), where the mass distribution is spherically symmetric and the velocity dispersion (σ) is isotropic. This gives ($\rho \propto r^{-2}$) for the right-hand side of an isothermal sphere ($V_{rot}^2 + \sigma^2$), Even so, minimum values of line-of-sight velocity may be obtained from a range of circular orbits of spherical shape at radius (r), as well as the virial rule extended to a uniform density sphere with fixed and isotropic velocity dispersion (implied by the solid-body rotation curves of the optical components of many dwarf galaxies) [17].

The galaxy's total mass, which seemed firmly established in the 1960s, has subsequently become a subject of considerable uncertainty. Calculating total mass out to the distance of the furthest large hydrogen clouds is straightforward. Velocities are low in the core parts of the system; because not much mass is inside the orbit of the gas clouds; they will be high at intermediate distances because most of the material is inside the orbit of the gas clouds in that scenario, and the gravitational pull inward is at its strongest. Because the clouds hold almost all the material, velocities drop dramatically over long distances [18].

1.5. Far infrared luminosity (L_{fir}) and blue optical luminosity (L_{opt})

The development of far-infrared diagnostics to determine the circumstances in infrared-bright galaxies, which are frequently interacting or merging galaxies is crucial for galaxy evolution research. Gas-rich galaxy interactions and mergers generate centrally focused, infrared-brilliant star formation, as well as veiled or partially obscured nuclear accretion activity via dissipative collapse, and play an important role in galaxy evolution [19].

Far-infrared wavelengths allow for the observation of dust-enshrouded galaxies without significant extinction effects, as well as several diagnostics of the physical conditions in their interstellar medium [20].

The far-infrared diagnostics improvement, which is regularly collaborating or blending galaxies, is critical for the investigation of cosmic system galaxy advancement. Far-infrared glow studies have now established a critical role in the development of massive galaxies in the Universe. Like far-infrared galaxies, the emission from youthful massive stars,

consumed via dust grains in their medium interstellar, is re-transmitted as warm continuum outflow at far-infrared frequencies [21] and contained in Table 2.

Far-infrared luminosity (L_{fir}) are given for (40–120) μm wavelength range [22]:

$$L_{fir} = 3.94 \times 10^5 \times D^2 \times (2.58 * f_{60} + f_{100}) \quad (5)$$

Here Far-infrared luminosity (L_{fir}) in unit (L_Θ). Where F_{60}μm and F_{100} μm are IRAS Far-infrared band fluxes at 60 μm and 100 μm in unit Jansky (Jy), where 1 J y= $10^{-26} W\ m^{-2} Hz^{-1}$ (in units SI) and listed in Table 2.

While Optical luminosity is still the most common and significant population tracer of the distribution of the volume density of galaxies. Optical luminosity was also the first tracer to be analyzed in specific since it has historically been easier to identify galaxies at optical wavelengths than in the radio spectrum [23].

The Blue optical luminosity (In optical band at 4400 A^0), (L_{opt}) are computed in unit solar luminosity (L_Θ) by Ref. [23]:

$$L_{opt} = D^2 \times 10^{12.193} \times 10^{-0.4 Btc} \quad (6)$$

where (Btc) is apparent B-mag corrected for galactic extinction internal extinction and k-correction, also listed in Table 2.

The basic data for sample data galaxies are given in Table 1 and it's organized per name galaxy as follows:

Column (1): names are given for each galaxy, taken from the NED (https://ned.ipac.caltech.edu/) survey.

Column (2): the other names of chosen sample galaxies, taken from the database and a collection of tools to study the physics of galaxies and cosmology HyperLEDA (http://atlas.obs-hp.fr/hyperleda/).

Column (3): Morphological type of irregular galaxies, the morphological type, or Hubble type, is coded from early to late types as: Io-IB-IB-IBm- IAB, from NED survey.

Column (4): log d_{25} in unit (arcmin) taken from HyperLEDA.

Column (5): d_{25} in unit (arcmin) calculated from: $d_{25} = 0.1 \times 10^{logd25}$

Column (6): Mean Heliocentric radial velocity is taken from HyperLEDA.

Column (7): Distance of galaxies (D) in unit (Mpc), calculated from "Eq. (1)" for our work.

Column (8): Linear diameter of galaxies (A_0) in unit (kpc), calculated from "Eq. (4)".

Column (9): total mass of irregular galaxies (M_I) in unit solar mass (M_Θ), taken from "Eq. (3)".

While Table 2 listed some physical properties of (70) sample Irregular Galaxies, as follows:

Column (2): the Apparent B-mag bt corrected for galactic extinction (btc) in unit (mag), taken from the database and a collection of tools to study the physics of galaxies and cosmology (HyperLEDA).

Column (3): This quantity is the physical maximum velocity rotation corrected for inclination (vrot), expressed in km/s, taken from HyperLEDA.

Column (4): Far-Infrared microns (f_{60}) in unit (Jy) taken from NED.

Column (5): the logarithm value of the infrared flux in (f_{60}) μm band in unit (Jy).

Column (6): far-infrared luminosity (L_{fir}) in unit (L_Θ), calculated from "Eq. (5)" for our work.

Column (7): the blue optical luminosity Optical (L_{opt}) in unit (L_Θ)), taken from "Eq. (6)".

2. Results

In this paper, statistical software (Microsoft Office Excel and STATISTICA) program was used to calculate, and investigate the relationship between several parameters (luminosity and mass).

Many regressions have been used to get a graph between these parameters. Investigation of an unbiased sample of active galaxies; with comprehensive observational data on relevant parameters at different wavelengths is essential for a statistically reliable test, for understanding the different physical conditions in these objects, and for testing the unification model.

In this research, methods were described to estimate, total mass $M_I(M_\odot)$, linear diameter A_0, far-infrared luminosity (L_{fir}) for $(40-120)\mu m$ wavelength range and blue optical luminosity (Optical at $4400A^o$) (L_{opt}) of irregular galaxies.

The statistical parameters are evaluated in this research to assess if there is a relationship between these parameters, like (total mass – far-infrared luminosity) and (total mass – blue optical luminosity). Besides, various regressions are employed in this paper to construct a plot between these variables.

All coefficients, including the distance effect, were measured between (L_{fir}, L_{opt}) bands for our sample set of irregular galaxies. As a consequence, the false connections between luminosities and totals caused by the fact that more effective sources detected at vast distances significantly decreased using this method.

Analysis and a calculation of (70) samples of data of irregular galaxies show that there is a relationship

between (total mass-rotation velocity), (total mass-linear diameter), and (total mass-angular diameter) (see Table 1). The overall measurement results between (far-infrared luminosity-blue optical luminosity) are summarizing in Table 2. A comparison produced of the relationship between irregular galaxies and milky galaxies is shown in Table 3. Table 4 shows the correlation coefficient (r) and probability of chance correlation (P) between various parameters of (70) sampled irregular galaxies.

Finally, the descriptive statistics of mean (average) variables and standard error for sample irregular galaxies are shown in Table 5.

Figs. 1 and 2 demonstrate the mathematical equations computed in this paper for this irregular galaxies type. As we can see from these figures in this work, the relationship of the parameters between the total mass, rotation velocity, and linear diameter of these galaxies.

The results of the analysis of our sample data of irregular galaxies show that the total mass and linear diameter are closely related, as shown in Figs. 1 and 2. On the other hand, the total mass and far-infrared luminosity, the total mass, and blue optical luminosity are closely related, as shown in Figs. 3 and 4. While Fig. 5 shows a clear linear association between (L_{fir} and L_{opt}), which could be associated with the recent formation of these galaxies.

3. Discussion

From this research, it is possible to conclude that multiple regression analysis gives two main points: the total mass of an irregular galaxy is correlated with its linear diameter and velocity. Second, for irregular galaxies the correlations between total mass, linear diameter and velocity are significantly steeper, and the mathematical relationship between them is a direct relationship $M_I(M_\odot)$, direct proportion with (A_0), (V_{rot}).

Our observations in this paper indicate that there is a strong connection between the curve rotation velocity and total mass, as shown in Fig. 1. The analysis of the ratio between mass and linear diameter is a direct relationship plotted in Fig. 2, a relationship and strong correlation between the irregular galaxy (M_I and L_{fir}) shown in Fig. 3. Likewise, there is a strong connection between the relationships (L_{opt} and M_I), as shown in Fig. 4. A clear linear association is obtained between (L_{fir} and L_{opt}), which could be associated with the recent formation of these galaxies, see Fig. 5.

The total mass of the Milky Way is $(1 - 1.5 \times 10^{11} M_\Theta)$ [1] according to Table 3, and the total mass of irregular galaxies is $(9.69 \times 10^9 M_\Theta)$ according to our work in this paper. Irregular galaxies have smaller sizes compared to the Milky Way, which is clear from Table 3. The study indicates that the ratio of the mass of the Milky Way to the mass of irregular galaxies is approximately (15) times greater than the sample of irregular galaxies. This is because the size of the spiral galaxy (and the Milky Way is a type of it) is greater than the irregular galaxies.

Also, in relation ($\log M_I - \log L_{\text{fir}}$) there is a clear relation with a positive and clear correlation coefficient ($r \approx 0.558$), for sample irregular galaxies there is a strong intrinsic correlation coefficient ($r \approx 0.815$) of the ($\log M_I - \log \text{Vrot}^2$) plot and $r \approx 0.7023$for relation ($\log M_I - \log L_{\text{opt}}$) as shown in Table 4.

The irregular galaxies, and because of their small size, the rotation velocity of these galaxies is greater than the Milky Way. And this is confirmed by our calculations in this paper, where we found that the average maximum rotational velocity (V_{rot}) corrected from the inclination of the irregular galaxies is $(64.4km)$, but the average rotation velocity (V_{rot}) of the Milky Way is $(24km)$ [1].

Also the calculations of our sample data, we found that the average value of the mean heliocentric radial velocity (V_H) of the irregular galaxy is $(740.43km/s)$; while the average value of the mean heliocentric radial velocity (V_H) of the Milky Way is $(229km/s)$ [17] as shown in Table 3 that has been obtained from the calculations in this research.

This study also revealed that the estimate of the ratio of the rotational velocity of the Milky Way to the rotational velocity of irregular galaxies is roughly equivalent to (0.3727), and on the other hand, the ratio of the mean heliocentric radial velocity of the Milky Way to the mean heliocentric radial velocity of irregular galaxies is roughly equivalent to (0.3093), because irregular galaxies do not have systems that slow down their speed, such as spiral arms and discs, which both are components of the Milky Way. So we estimate the ratio of the rotational velocity of the Milky Way to the rotation velocity of irregular galaxies, which is roughly equivalent to (0.3727).

From Table 3, we found the ratio (V_H) of the Milky Way to (V_H) [25] of irregular galaxies is roughly equivalent (0.3093) for the sample data of irregular galaxies, because irregular galaxies don't have systems that slow down their speed, like don't have spiral arms and discs, which both are components of the Milky Way.

Finally, the values of far-infrared luminosity (L_{fir}) [and the blue optical luminosity (L_{opt}), are $(6 \times$

$10^8 L_\Theta$), and (3×10^9) [26] respectively that appear in the Table 3 for irregular galaxies. They were less than the average values of far-infrared luminosity (L_{fir}) and the blue optical luminosity (L_{opt}), which are ($8 \times 10^9 L_\Theta$) and ($3 \times 10^9 L_\Theta$) respectively for the our galaxy (Milky Way), where are calculated from the previous equations in this paper, and the reason for that is due to the dust that contains in the irregular galaxies, in addition to being newly formed.

4. Conclusion

This work investigated a statistical analysis of the physical properties of the (70) samples from the database and a collection of tools to study some physical parameters of irregular galaxies (HyperLEDA) and the NASA/IPAC Extragalactic Database (NED) survey. Our reviews can be concluded by focusing on the following main points:

1) The total mass of irregular galaxies is related to a linear strong relationship with the linear diameter and heliocentric radial velocity V_H.
2) Irregular galaxies are commonly small, so we found the total mass of irregular galaxies is ($9.69 \times 10^9 M_\Theta$), about one-fifteenth of the mass of the Milky Way galaxy because they have no spiral or bulge center. Thus, due to their small sizes, they are flat to effects substantial like collapsing with massive galaxies and intergalactic clouds.
3) We have demonstrated the irregular galaxies take on no shape, it's not easy to measure them, but on average they are almost $5.6Kpc$ in linear diameter, and because of their small size, the rotation velocity of these galaxies is greater than the Milky Way.
4) We have shown that the mean of blue optical and infrared luminosities of irregular galaxies ($3- 6\times 10^8 L_\Theta$) are very bright and bluer, which is a result of the gas and dust in them. This gas and dust is formed by many stars within an irregular galaxy, giving them their brightness, but not as much as the Milky Way galaxy.
5) Lastly, we have found the ratio of the radial velocity (V_H) of the Milky Way to (V_H) for irregular galaxies is roughly equivalent to (≈ 0.3), and the ratio of the rotational velocity of the Milky Way to the rotation velocity of irregular galaxies is roughly equivalent to (≈ 0.4), which means that irregular galaxies have neither a bulge nuclear nor any trace structure of spiral arms and discs.

Acknowledgments

The authors are grateful to Assistant Prof. Dr. Mohammed Naji for his moral support. Many thanks to the University of Baghdad/ College of Science/ Department of Astronomy and space for its support to finish this paper. Special thanks to the anonymous reviewers for their valuable suggestions and constructive comments.

References

[1] P.H. Karttunen, Fundamental Astronomy, Springer Heidelberg, New York Dordrecht, London, 2016.
[2] M.R. Sultanova, Automatic Approach to Mmorphological Classification of Galaxies with Analaysis of Galaxy Populations in Clusters, Doctor Thesis, University of North Dakota, Grand Forks, North Dakota, 2018.
[3] M. Povíc, Development in astronomy in Ethiopia and East-Africa through nuclear activity ingalaxies, Science 1 (2020) 1−5.
[4] M.N. Al Najm, Y.E. Rashed, H.H. AL-Dahlaky, Studying the flux density of bright active galaxies at different spectral bands, Science 16 (2019) 230−236.
[5] Y. Sofue, Rotation and mass in the Milky Wayand spiral galaxies, Publ. Astronom. Soc. Jpn. 1 (2016) 1−34.
[6] H. Parvathy, Rotation Curves of Galaxies, Maraimalai Campus, Guindy, MastersThesis, Submitted to Indian Institute of Technology Madras, 2015.
[7] T.-Y. Cheng, C.-J. Conselice, A.−A. Salamanca, N.-L. Bluck, W.-G. Hartley, J. Annis, D. Brooks, P. Doel, J.-G. Bellido, D.-J. James, K. Kuehn, N. Kuropatkin, M. Smith, F. Sobreira, G. Tarle, Optimising automatic morphological classifcation ofGalaxies with machine learning and deep learning usingDark energy survey imaging, Aastro-ph. 1 (2020) 24.
[8] K.L. Sarah, The Cosmic Evolution of Star-Forming Galaxies, Doctor Thesis, Natural Sciences submitted Combined Faculties of the Natural Sciences and Mathematics of the Ruperto-Carola-University of Heidelberg, Germany, 2019, p. 2.
[9] M. Das, S. Mcgaugh, R. Ianjamasimanana, K.-S. Dwarakanath, Shield: neutral gas kinematics and dynamics, Astrophysical 6 (2016) 53.
[10] M. Das, S. Mcgaugh, R. Ianjamasimanana, K.-S. Dwarakanath, J. Schombert, Tracing the dynamical mass in galaxy disks using HI velocity dispersion and its implications for the dark matter distribution in galaxies, Astrophys. J. 1 (2019) 13.
[11] R. Swaters, M. Balcells, The Westerbork HI survey of spiral and irregular galaxies, Astron. Astrophys. 1 (2002) 1−18.
[12] R. Rekola, Distance determinations, to nearby galaxies, Doctoral dissertation, Finland, Turku, 2004.
[13] E. Rashed, M.N. Al Najm, H.H. Al Dahlaki, Spectral multi-avelength properties of a RBSC- NVSS observation for a sample of active galaxies, Sciences 9 (2018) 15729−15740.
[14] M.A. Najm, Studying the atomic and molecular hydrogen mass (MHI, MH2) properties of the extragalactic spectra, Science 61 (2020) 233−1243.
[15] Y. Sofue, Invited Review the GALEX in the Milky Way and Spiral Galaxies, vol. 69, 2017, pp. 1−35.
[16] U. Dudzevici, I. Smail, A.-M. Swinbank, C.-F. Lim, W.-H. Wang, J.-M. Simpson, C.-C. Chen, D. Clements, H. Dannerbauer, L.-C. Ho, H.-S. Hwang, C.-H. Lee, D. Scott,

H. Shim, R. Shirley, Y.- Toba, Tracing the evolution of dust-obscured activity using sub-millimetre galaxy populations from STUDIES and AS2UDS, MNRAS 1 (2020) 20.

[17] G.-L. Hoffman, E.-E. Salpeter, B. Farhat, T. Roos, H. Williams, G. Helou, Arecibo hi mapping of a large sample of dwarf irregular galaxies, Astrophysical 105 (1996) 30.

[18] E. Gregersen, The milky way and beyond, in: Association with Britannica Educational Publishing, Rosen Educational Services, 2010.

[19] J. Fischer, N.-P. Abel, E.-G. Alfonso, C.-C. Dudley, S. Satyapal, P.-A. van Hoof, A far-infrared spectral sequence of galaxies: trends and models, Astrophysical 795 (117) (2014) 24.

[20] J.R. Brauher, D.A. Dale, G. Helou, Compendium of far-infrared line and continuum emission for 227 galaxies observed by the infrared space observatory, Science 1 (2008) 1−95.

[21] F. Casoli, J. Dickey, I. Kazes, A. Boselli, P. Gavazzi, K. Baumgardt, H1, H2 and star formation in galaxies in the region of the coma supercluster, Astron. Astrophys. 309 (1996) 43−58.

[22] Z. Butcher, S. Schneider, W. van Driel, M.-D. Lehnert, Bivariate luminosity-Hi mass distribution function of galaxies based on the NIBLES survey, A&A 619 (2018) 1−14.

[23] A. Sipols, A. Pavlovich, Dark Matter Dogma: A Study of 214 Galaxies, Galaxies 8 (2018) 1−32.

[25] T.C. Licquia, J.A. Newman, J. Brinchmann, Unveiling the milky way: a new technique for determining the optical color and luminosity of our galaxy, Astrophys. J. 809 (2015) 1−19.

[26] D. hovmann, D. Lemeke, C. Thum, Surface brightness of the central region of milky way at 2.4 and 3.4 mm, Astron. Astrophys. 57 (1977) 111−114.